

Robust Stimulus Encoding in Olfactory Processing: Hyperacuity and Efficient Signal Transmission

Tim Pearce,¹ Paul Verschure,² Joel White,³ and John Kauer³

¹ Department of Engineering, University of Leicester, University Road LE1 7RH, United Kingdom. t.c.pearce@le.ac.uk

² Institute of Neuroinformatics, University/ETH Zürich, CH-8057 Zürich, Switzerland. pfmjv@ini.phys.ethz.ch

³ Department of Neuroscience, Tufts University Medical School, Boston, MA 02111, USA. jwhite@opal.tufts.edu jkauer@opal.tufts.edu

Abstract. We investigate how efficient signal transmission and reconstruction can be achieved within the olfactory system. We consider a theoretical model of signal integration within the olfactory pathway that derives from its convergent architecture and results in increased sensitivity to chemical stimuli between the first and second stages of the system. This phenomenon of signal integration in the olfactory system is formalised as an instance of hyperacuity. By exploiting a large population of chemically sensitive microbeads, we demonstrate how such a signal integration technique can lead to real gains in sensitivity in machine olfaction. In a separate computational model of the early olfactory pathway that is driven by real-world chemosensor input, we investigate how spike-based signal and graded-potential signalling compares for supporting the accuracy of reconstruction of the chemical stimulus at later stages of neuronal processing.

1 Introduction

The olfactory system provides an ideal model to consider the issues of robust sensory signal transmission and efficient encoding/decoding within neural systems. It must overcome large shifts in operating conditions occurring over time, that together add up to a continual state of flux at its periphery, the olfactory epithelium. A key constraint is that the main sites for chemical transduction, Olfactory Receptor Neurons (ORNs), are in a rapid and continuous state of development and programmed apoptosis (at least in mammals) which differentiates them from all other sensory neurons within the nervous system[1]. This neurogenesis means that the total number of receptors innervating the first point of signal processing, the olfactory bulb, fluctuates over time as signals from degenerating ORNs cease and axons from large numbers of newly formed ORNs make their way to integration sites called glomeruli. How this is achieved is a fascinating and recently uncovered story of axonal guidance [2] but in the context of robust stimulus encoding we are primarily interested in the effect of this

turnover of receptors on signal transmission. The key issue here is how the olfactory system manages to cope with changing numbers of receptors, yet still generate a consistent signal to support odour perception over time.

Another factor of crucial importance when considering robust signal processing in the olfactory system is evidence suggests that not only do the numbers of receptors change as a result of neurogenesis, but also shifts in the response characteristics of ORNs occur during the act of perception. Receptor adaptation or fatigue is a key factor here and is known to occur in ORNs as their response adapts strongly during exposure to high levels of specific chemicals or repeated exposure[3]. Since the olfactory system relies on an entire population of broadly-tuned chemosensors (of which there now appears to be around a thousand in mice, fewer in fish [4]) these shifts in tunings may play a fundamental role in determining the stability of the system as a whole, and so this provides another perspective from which to consider robust signal transmission and processing within the olfactory pathway.

Signals from ORNs must be transmitted over relatively large distances from the olfactory epithelium at the top of the nasal passages, through the cribriform plate, and into the olfactory bulb where they are integrated at the glomeruli. In general, action potentials are used within the nervous system to encode and represent the stimulus between the transducer and first site of processing. This encoding strategy possesses robust noise-resistant properties that result from its intermittent discretised nature [5] that will be considered later in this chapter. Astonishingly the system solves this transmission problem as well as improving sensitivity at the first stage of processing over and above that obtained at the receptor level. We will formalise this phenomenon as an instance of hyperacuity.

These shifts in operating conditions have a direct impact on the reliable processing of sensory information within the olfactory pathway since it must overcome constant change and external noise sources in order to maintain a robust capability for characterising and discriminating complex mixtures of molecular stimuli. Despite changes in both receptor numbers and their characteristics, odour perceptions are remarkably stable with time (subject to respiratory infection of course). The ability of the olfactory system to achieve robust performance in the face of such a high degree of change appears to derive principally from its neuronal architecture in combination with the signal encoding strategies employed, as we will discuss here.

We will consider two models of the early stages of the olfactory pathway that speak to the issue of how a robust signal representing the stimulus is transmitted to the first stages of processing and how the quality of the signal is maintained during this process. Specifically, the first model will provide a probabilistic interpretation of signal integration of receptor signals at glomeruli, which predicts a lowering of detection limits at the system level compared with individual receptors. This signal integration model will be tested experimentally by applying it to data obtained from real-world chemosensor microbeads that mimic key properties of olfactory receptors. In the second model, the issue of signal transmission within the early stages of the olfactory pathway will be addressed, by

comparing an action-potential based model with one mediated by graded-voltage signals. This allows us to investigate under which operating conditions the signal integrity is maintained at each glomerulus.

A number of questions will be addressed using these models. For example, can signal integration at the glomerulus account for sensitivity enhancement observed in the biology? Is it reasonable to consider sensitivity enhancement within the olfactory system as an instance of hyperacuity, and if so then how should this be quantified? Also, how does spiking and graded signal encoding affect signal integrity within the early stages of olfactory processing?

Our models are simple, yet capture what we believe to be the key features of the early olfactory pathway; they are population-based, probabilistic, and spiking. This enables us to better understand the biology by making predictions about the performance of alternative coding and processing schemes that can be reasonably hypothesised, such as comparing spiking and graded-voltage signal transmission.

The models we consider are implemented as part of a biologically plausible artificial nose, which is driven by real-world optical microbead chemosensor input. The sensors have a number of properties similar to biological olfactory receptors and prove ideal for implementing functional models of the biological olfactory pathway. It is possible to operate the signal processing models and these sensing elements in combination and in real-time to comprise an artificial olfactory system[6]. Consequently, research in this area can inform us not only about neuronal information processing within biological systems but also on how to achieve better design in the field of machine olfaction.

After discussing the implications of our models for robust signal processing we will conclude this chapter with a discussion of how signal encoding and processing strategies within the olfactory system may inform more general architectures for computation that are based upon emerging results in neuroscience.

2 Receptor Convergence and Olfactory Hyperacuity

A marked feature of the mammalian olfactory system is the massive convergence of spiking receptor input from thousands of olfactory receptor neurons onto glomeruli, the first stage of processing in the olfactory bulb[4]. This convergence appears to be fundamental to the operation of the olfactory system since it is conserved across many species. This arrangement raises the question of how reliable odour encoding can be achieved in view of large numbers of discretised receptor inputs that converge onto the olfactory bulb?

We contend that one consequence of the massive convergence of sensory input [7] within the olfactory bulb is sensitivity enhancement. This arrangement is schematised in Fig. 1 where n receptors (n being in the order of 2-10 thousand in mammals) expressing the same receptor protein(s) generally converge onto two glomerular regions[8]. In the simplest scheme, we can consider the spike-trains generated by individual receptors as statistically independent Poisson processes

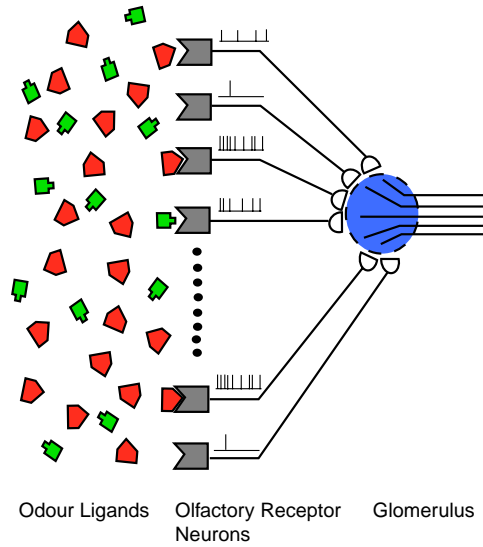


Fig. 1. A schematic of receptor convergence at the early stages of the mammalian olfactory pathway. Odour molecules are thought to interact with putative 7-transmembrane domain receptor proteins within the hair-like cilia of Olfactory Receptor Neurons (ORNs) leading ultimately to the generation of an action potential. The vigour of the cell response depends on both the suitability of the ligand to activate the second-messenger cascade signalling pathways and also the number of ligand-receptor interactions occurring at a specific cell. Action potentials produced by ORNs propagate over relatively large distances to reach the glomeruli of the olfactory bulb, which act as common sites for integration.

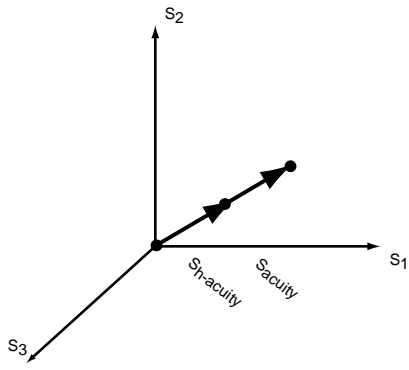


Fig. 2. A simplified representation of odour space in which each axis corresponds to a separate chemical component – the distance along each axis corresponds to its concentration. Since many simple odour compounds exist, this state space will be of high dimensionality and contain significant redundancy, since many permutations of odour concentration will never occur in the natural world. Any given point in odour space represents a complex mixture of volatile compounds with a unique fingerprint of relative concentrations, that elicits a specific perceived odour quality. The vectors demonstrates the just noticeable difference (jnd) in the stimulus that is required to either detect a difference from a single chemoreceptor, s_{acuity} , within the olfactory system or psychophysically as reported perceptually, $s_{h-acuity}$.

(after Van Drongelen *et al.* [9]), where the probability of observing ($N = X$) action potentials within a time-window, δt , is governed by the Poisson distribution

$$P_r(N = X) = \frac{\lambda_r^X}{X!} e^{-\lambda_r} \quad (1)$$

where $\lambda_r = k_s \delta t$ and k_s is the mean firing rate expected for each stimulus, s . Since olfactory receptors probably have different ranges of tuning to particular stimuli, we would expect k_s to vary for a particular receptor over a given test-set of odorants. However, one effect of convergence of receptor input at the glomerulus might be to aggregate multiple spike-trains over a period of time. So while the statistics of spike generation at the receptor level may be governed by λ_r , at the glomerulus, $n\lambda_r$, spikes are expected on-average in time-window, δt . The spiking input to each glomerulus is considered as another Poisson process, but now with time-constant $\lambda_g = n\lambda_r$. The signal-to-noise ratio (SNR) enhancement of this convergent architecture is derived from the dispersion of the aggregated signal at the glomerulus, λ_g , compared with that of the individual receptor spike-trains, λ_r , so

$$\text{SNR} = \frac{\sigma_g}{\sigma_r} = \left(\frac{\lambda_g}{\lambda_r} \right)^{1/2} = \left(\frac{n\lambda_r}{\lambda_r} \right)^{1/2} = \sqrt{n} \quad (2)$$

and we expect an enhancement in sensitivity to follow \sqrt{n} , with increasing receptor numbers, n . This is a form of hyperacuity where the biology takes advantage of the statistics at the receptor level in order to generate overall system sensitivity that is greater than that of the underlying detectors.

There can be many forms of hyperacuity within a single sensory modality. For example, within the visual system three forms are commonly discussed; colour perception, vernier-style hyperacuity, and stereo-optic depth perception[10]. In each case the overall perceptual performance has been measured empirically using psychophysical experiments and then compared with theoretical physical limits imposed on the sensory system, such as receptor spacing or diffraction limits imposed by the optics of the eye. The point at which acuity becomes hyperacuity can be measured empirically when the overall psychophysical detection limits exceed those calculated from physical constraints placed on the sensory system or as measured electrophysiologically at the receptor level.

Probably the most widely studied example of hyperacuity in the visual system is during the perception of relative spacings in the visual field in two dimensions at the plane of fixation – so-called vernier-style hyperacuity. The effect can be measured empirically using a wide range of psychophysical experiments, a well known example being the estimation by an observer of relative spacing between four parallel lines on a plain background, studied by Klein and Levi (1985)[11]. By varying the spacing between the lines by minute amounts they managed to test the acuity of the visual system in detecting relative displacement shifts in the visual field. To demonstrate hyperacuity in this context requires the just noticeable difference (jnd) in the displacement between the lines, as reported by the observer, which gives rise to a small displacement of the projected image

onto the retina, to be far smaller than the receptor spacing. Klein and Levi measured the perceptual thresholds to be *ca.* 0.9 seconds of arc, whereas the receptor spacing on the retina is *ca.* 30 seconds of arc[11].

While hyperacuity may confound our intuition regarding detection limits in the biology, it becomes far less baffling when considered in a statistical sense. For the example of relative line spacing in the visual field, the signals from many more than a single receptor can be called upon to solve the task. By recruiting the signals from a population of receptor cells it is possible to surpass the detection limits to which individual receptors are subject. Population coding and hyperacuity can be considered to be closely related phenomena.

Within the olfactory system, at first glance there appears to be two very separate forms of hyperacuity present. The first of these relates to sensitivity enhancement, formalised above. Here, ORNs expressing identical single receptor proteins (or combinations thereof) aggregate their signals at common sites, resulting in an overall jnd to a preferred compound that exceeds that of individual chemoreceptors. We may refer to this as a kind of concentration hyperacuity, which may be quantified by comparing reported detection thresholds obtained from psychophysical or electrophysiological experiments conducted using pure odour compounds with those thresholds observed at the individual receptor level using single-unit recordings. Another form of olfactory hyperacuity can be considered to arise from the combined action of a broadly tuned population of ORNs. By combining signals from many ORNs expressing different receptor proteins, the later stages of the olfactory pathway may enhance discrimination between similar complex odour stimuli over and above that achievable by any single chemoreceptor type. We may refer to this as a form of odour quality hyperacuity which may be quantified by comparing ORN single-unit recordings in response to paired odour stimuli for their ability to account for discrimination of the same odour pair as reported psychophysically or measured electrophysiologically.

Consideration of the underlying neuronal architecture uncovers just how closely related these two forms of hyperacuity might be. For example, overlapping receptor tunings also contribute to lower detection limits to single compounds and so it is not possible to attribute the phenomena of sensitivity enhancement to a single receptor type. Similarly, convergence of single receptor types also supports better multicomponent odour quality discrimination within the olfactory system and so single receptor types make significant contribution to encoding quality. Also note that in this context odour quality and quantity are not entirely separable since changes in concentration of some odour compounds are known to have marked effects on the perceived odour quality. A single definition of olfactory hyperacuity might suffice that avoids this awkward distinction. As a working definition consider

Olfactory hyperacuity is demonstrated by the discrimination of two chemically different odour stimuli (which may vary in both quantity and quality) observed at the later stages of the olfactory pathway and mea-

sured either psychophysically or electrophysiologically, that cannot be accounted for by any single underlying chemosensor.

Notice that this definition is broad enough to encompass many olfactory scenarios – in particular changes in both odour intensity and quality. Fig. 2 shows an odour space representation, which provides an intuitive understanding of this definition for olfactory hyperacuity. Here, each point in odour space has an associated odour perception, the quality of which varies with changes in the relative concentration between the components of a complex odour mixture. The nearest excursion from a given point in odour space that produces a shift in the reported perception corresponds to the jnd in the stimuli that can be recognised – vector $s_{\text{h-acuity}}$. The excursion that demonstrates a statistically significant change in response at the single-unit level represents the jnd for that particular ORN – vector s_{acuity}^i for receptor class i . To demonstrate olfactory hyperacuity, the magnitude of jnd observed at the perceptual level must be far smaller than for any underlying receptor

$$|s_{\text{h-acuity}}|_2 \ll |s_{\text{acuity}}^i|_2 \text{ for all } i, \quad (3)$$

where $|\bullet|_2$ is the usual l -2 Euclidean norm.

Hyperacuity of this form has already been demonstrated within the olfactory system through electrophysiological measurements in both mammals and insects. Duchamp-Viret *et al.* (1989) measured sensitivity enhancement to a variety of single odour ligands at both the receptor and olfactory bulb level in the frog[12]. Their results show a clear lowering of the detection limits at the bulb level when compared with that observed for the underlying receptors. Interestingly, this effect is observed only when a large portion of the olfactory mucosa is exposed, compared with a punctate delivery to the receptor sheet. This provides further evidence that hyperacuity in the olfactory system relies upon the recruitment of a large population of receptors. Given that the convergence ratio of receptors onto glomeruli in the frog is similar to other small mammals and estimated to be *ca.* 1000 [12, 13] the theoretical model of hyperacuity at the front-end of the olfactory system, represented by (2), predicts a lowering of the detection limit by a factor of *ca.* 32. In support of this prediction, Duchamp-Viret and co-workers observed between 1-2 orders of magnitude sensitivity enhancement in their measurements[12].

Similar measurements in the antennal lobe of cockroach have been made by Boeckh and co-workers demonstrating spectacular sensitivity enhancement to pheromone compounds - regularly between 1-4 orders of magnitude but also as high as six orders of magnitude between measurements taken at the antennae and the Macroglomerular Complex (MGC) of the antennal lobe[14]. These results are intriguing since although high convergence ratios of ORNs onto specialised glomeruli in the MGC of insects have been reported, these are nowhere close to the enormous convergence ratios required to support such extreme hyperacuity (10^{12} :1 receptor:glomeruli convergence ratios). Alternative mechanisms must be involved in enhancing sensitivity to such a high degree – one example of which might be noise-shaping[15].

The early stages of the olfactory pathway not only ensures efficient and robust signal transmission from the transduction sites to the first stage of processing, but clearly lower the overall system detection limits in the process. This provides only one example of how the convergent architecture of the olfactory pathway can teach us valuable lessons about robust signal processing within neural systems as it maintains high levels of sensitivity to relevant stimuli.

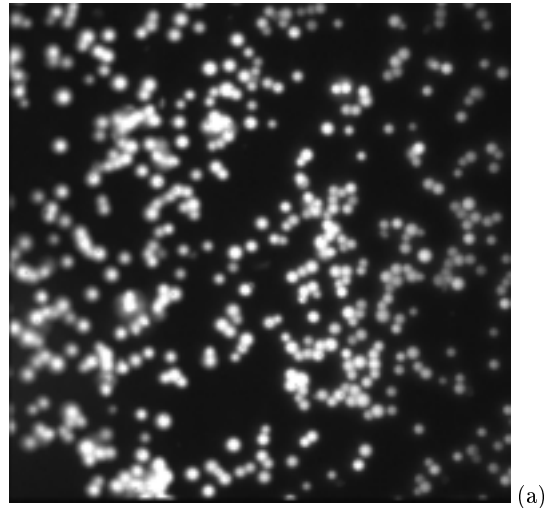
3 Hyperacuity in an Artificial Nose

Can we demonstrate such sensitivity enhancement within practical chemical sensing technology using the mechanism of hyperacuity in the olfactory system as a model? Even though artificial nose systems typically rely on arrays of widely tuned non-specific chemosensors, numbers of individual sensing elements are usually restricted overall, to reduce both system complexity and implementation costs. As a consequence it has not been possible to exploit the statistical properties of large numbers of chemosensor elements, simply due to lack of sensor numbers, as has been successfully exploited in the biological olfactory pathway to boost detection limits.

Optical microbead sensor technology, as depicted in Fig. 3a is ideally placed for such neuromorphic implementation. Enormous populations of microbeads may be deployed in a small area (the diameter being *ca.* 30 μm), from which the signal produced by each sensor element can be addressed individually. Only in such an arrangement can the issues of population coding in chemical sensing be addressed realistically. Individual microbead sensors are broadly-tuned to a wide range of organic compounds and so are reminiscent of the wide ranging but preferentially tuned responses observed in ORNs[16]. It is possible to effectively tune these devices by choosing different polymer/dye combinations so as to replicate to some extent the diversity of receptor types present in the biology. The devices are also small and low-power – a 3mW output laser-diode assembly can energise billions of optical microbeads in tandem, making it a useful chemical sensor technology in its own right[17].

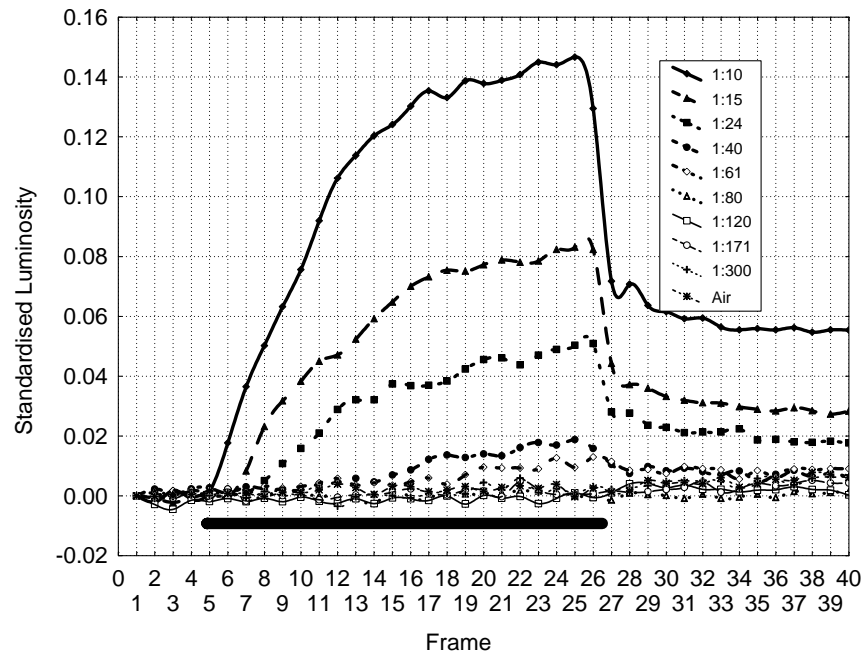
Our aim, then, is to investigate the statistics across a population of identical optical microbeads in order to test for evidence of olfactory hyperacuity as demonstrated in the biology. This would provide both a practical method for sensitivity enhancement in chemical sensing instrumentation as well as add credence to the biological model discussed in Sect. 2.

For this work 201 optical microbeads with similar response characteristics were imaged on a glass slide as these were exposed to different dilutions of the saturated vapour headspace of a single chemical compound – toluene. Fabrication details for the microbeads have been reported elsewhere[18]. The fluorescence response of each bead is sensitive to different chemicals in the microenvironment surrounding that sensor and can be imaged using a simple optical arrangement based upon a cooled CID camera and microscope lens similar to that described by White *et al.* [19] Odour delivery was achieved using an air-dilution olfactometer to apply pulses of analyte vapour to region of beads being imaged. A make-up carrier flow of ultra zero grade air was controlled at varying flow-rates to act as a diluent for the saturated vapour headspace



(a)

Example Single Bead Response



(b)

Fig. 3. (a) A grey-scale image showing 201 fluorescent microbeads responding to saturated toluene vapour at a single point in time. (b) A single bead response to different air dilutions of saturated toluene vapour over time, indicating concentration discrimination down to 1:61 dilution. The data were standardised by taking the average greyscale value for each individual bead and for each frame subtracting the greyscale value of the respective bead on the first frame of the sequence and finally dividing the result by the same first frame value. This results in a fractional pre-processing metric. The solid black line indicates odour exposure.

of toluene (*ca.* 3800 ppm concentration). Dilutions achieved using this odour delivery arrangement ranged between 1:10 to 1:300, corresponding to $154.8 \text{ nmol ml}^{-1}$ and 5.2 nmol ml^{-1} respectively.

Using this arrangement it was possible to image large numbers of these beads within a single CCD-frame - in this experiment 201 beads in total. The luminosity response of each bead to the analyte (across a small bandwidth in the fluorescent emission spectrum, 10 nm) may be accurately assessed by measuring the grey-scale levels around localised points in the image. After storing the individual bead responses during exposure to different concentrations of analyte over time, the statistics of the responses across the bead population were investigated.

The graph of Fig. 3b shows the variation in standardised luminosity over time for an individual microbead responding to different dilutions of saturated toluene vapour. The beads show a well defined response to a wide range of organic compounds that are both reversible and reproducible during repeated exposures. Clearly, the magnitude of the response is related to the concentration of the analyte and so the task is to be able to discriminate between the single analyte at different dilutions. A close inspection of the responses shown in Fig. 3b shows that for this particular bead, reliable discrimination was only possible down to the 1:61 dilution level. Below this concentration level the luminosity signal is seen to descend into the background noise.

To be able to demonstrate hyperacuity we must show that the discrimination capability of the population of microbeads surpasses that of a single bead. The best way to quantify the response of the bead population is statistically. From preliminary experiments with very high bead numbers (> 1000) the distribution of luminosity values, y obtained from a single bead population was found to closely match the Laplace (or double exponential) probability density function (pdf) at any particular point in time

$$p(y) = \frac{1}{2\beta} \exp\left(\frac{-|y - \mu|}{\beta}\right) \quad (4)$$

where β is the scale parameter determining the dispersion, μ is the mean, and the variance is given by $\sigma_y^2 = 2\beta^2$. The statistics of the population can be used to make a more accurate assessment of the true concentration of the analyte using fundamental concepts from signal detection theory.

Given a single bead measurement, y , we can assign it to the most likely dilution class, H_i , by maximising the a posteriori probability $p(H_i|y)$. In the case of equally likely dilution classes, it is simple to show using Bayes rule that this is equivalent to maximising the conditional probability, and so our decision rule reduces to (for two classes, H_1 and H_0)

$$\text{if } p(y|H_1) > p(y|H_0) \quad \text{choose } H_1, \text{ otherwise choose } H_0 \quad (5)$$

This decision process is depicted in Figure 4a, showing how the overlapping distributions of two signals can be used to assign the most probable class membership. Exactly the same approach is used here for a number of dilution classes. By fitting a distribution of the form given by (4) to the bead responses to each

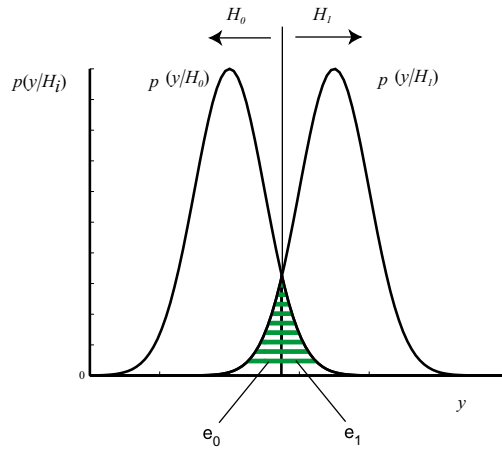


Fig. 4. The detection of two signals with distinct Probability Density Functions (pdfs). Using a threshold function it is possible to minimise the likelihood of making an error in assigning a hypothesis, H_0 or H_1 , to observation y . The areas ϵ_0 and ϵ_1 represent the probability of making this error.

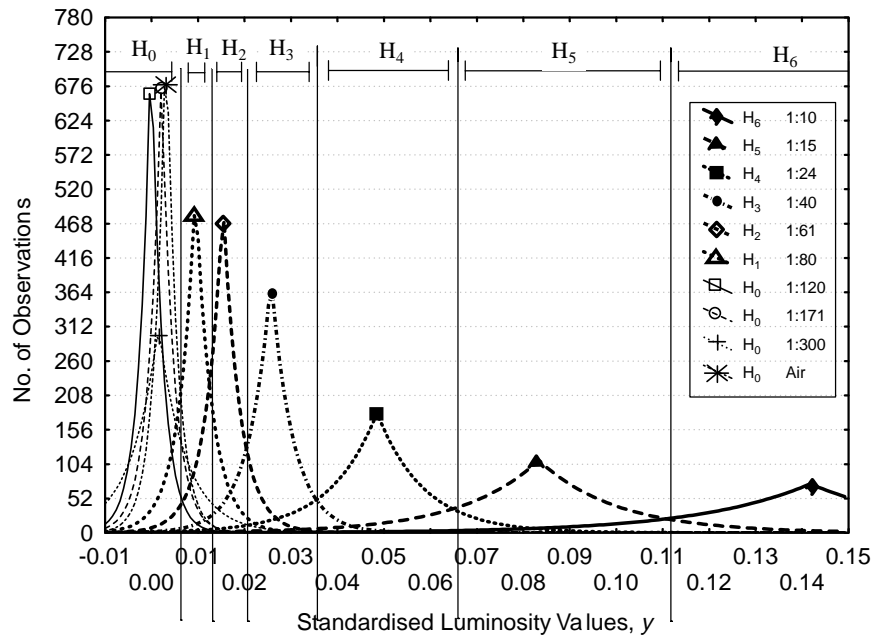


Fig. 5. Best fit Laplace distributions to the microbead population response to a variety of dilution categories. Distinct pdfs are observed down to 1:80 dilution taken at frame 25 where the bead luminosity response is maximum. The figure demonstrates how the expected value (the peak) of each distribution provide a far more accurate and robust measure of the actual dilution class - this being the basis of sensitivity enhancement in our artificial nose.

dilution the power of this discrimination scheme becomes clear. Figure 5 shows the multiple Laplace pdfs for each of the dilutions analysed. This can be used to make an optimal dilution class assignment for a single bead response to an unknown dilution of the analyte. Some overlap exists between the fitted pdfs, and so a level of risk must be tolerated in making this assignment. However, it is also clear from the distributions that the expected value (mean) across the bead population in each case provides a far more accurate estimator of the dilution category than any single bead response – which is the central issue in any hyperacuity effect. This can be quantified by the standard error in the mean, σ_μ which measures how much variation can be expected in the expected value of the distribution given by (4) when, n multiple samples are taken from a bead population.

$$\sigma_\mu = \frac{\sigma_y}{\sqrt{n}} = \frac{2\beta^2}{\sqrt{n}} \quad (6)$$

so while a single bead response is subject to variance $2\beta^2$ the variance of the mean taken from n independent and identically distributed bead responses is $\frac{2\beta^2}{\sqrt{n}}$.

We can also quantify this effect by estimating the SNR between the aggregated bead response of the population to the odour applied at a specific dilution (an estimate of the expected value $\hat{\mu}_{Hi}$) with the same population responding to air, $\hat{\mu}_{H0}$. It can be shown that the SNR between these two estimates of the mean can be calculated using the Student's t-test statistic[20]

$$\text{SNR} > t_{\alpha,\nu} \quad (7)$$

where the degrees of freedom $\nu = 2n - 2$, n is the number of microbeads within the population, and α gives the significance level required for the SNR estimate (taken here as $\alpha = 0.05$). After applying a t-test statistic it was possible to estimate how the SNR of the aggregated signal varied with differing numbers of beads – as shown in Fig. 6. The results show clear agreement with the SNR enhancement predicted by the biological model and demonstrate how olfactory hyperacuity may be implemented within an artificial nose to achieve sensitivity enhancement.

Figure 6 may also be used to estimate the number of beads required to reach a particular system detection limit and so solve a specific odour detection problem. Assuming a minimum SNR of 3 for reasonable detection, it is clear from extrapolating the characteristics that the 1:171 toluene dilution odour detection task could be solved with *ca.* 500 concurrent bead measurements and the 1:300 task with *ca.* 1,300 bead measurements.

4 Stimulus Encoding in the Olfactory System

Another issue of interest when considering robust signal processing within neural systems is how sensory signals are encoded in the CNS. It appears that a wide

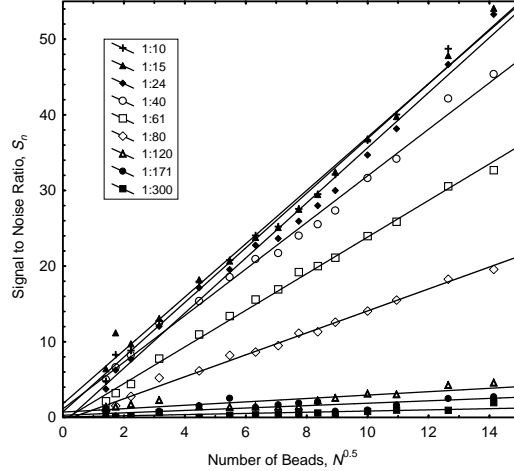


Fig. 6. Variation in the estimated SNR for a population of microbeads with different dilutions of analyte and bead numbers, \sqrt{n}

range of encoding strategies are employed by the biology in order to efficiently transmit sensory information under a wide range of conditions. Examples of coding strategies include graded potentials (usually over short distances), action potentials, rate codes, and specific temporal codings.

The key method of signal transmission between the first two stages of the olfactory pathway is known to be action potentials. Although these spiking signals are known to provide an efficient mechanism for long-distance transmission in the nervous system, how it can provide the signalling basis for reliable and accurate stimulus encoding is still debated[21, 22]. One approach to address this issue is to investigate different stimulus encoding schemes within computational models. In this section, we investigate the mass action of sensory input to a simple olfactory model that is driven by optical chemosensors to understand its behaviour in what has been termed a high-input regime[23].

In this context realistic chemosensory input derived from optical microbead input confers advantages in terms of more natural statistics of sensory input than can be achieved with a small number of sensors or simulated input. Accordingly, we can investigate the behaviour of our model under a probabilistic, high-input regime akin to the biology.

We applied the data-set shown in Fig. 3b to a simple model of the front-end of the olfactory system. The layout for the model is shown in Fig. 7a where data from each individual bead is mapped onto a series of cell populations in a 1-to-1 fashion. To address the stimulus encoding issues we consider here it is reasonable to connect a single simulated glomerular "cell" to a population of ostensibly identical fluorescent beads, to model the convergent architecture discussed in Section 2. In order to closely follow the biology of the system, the baseline response of the bead data was applied to a

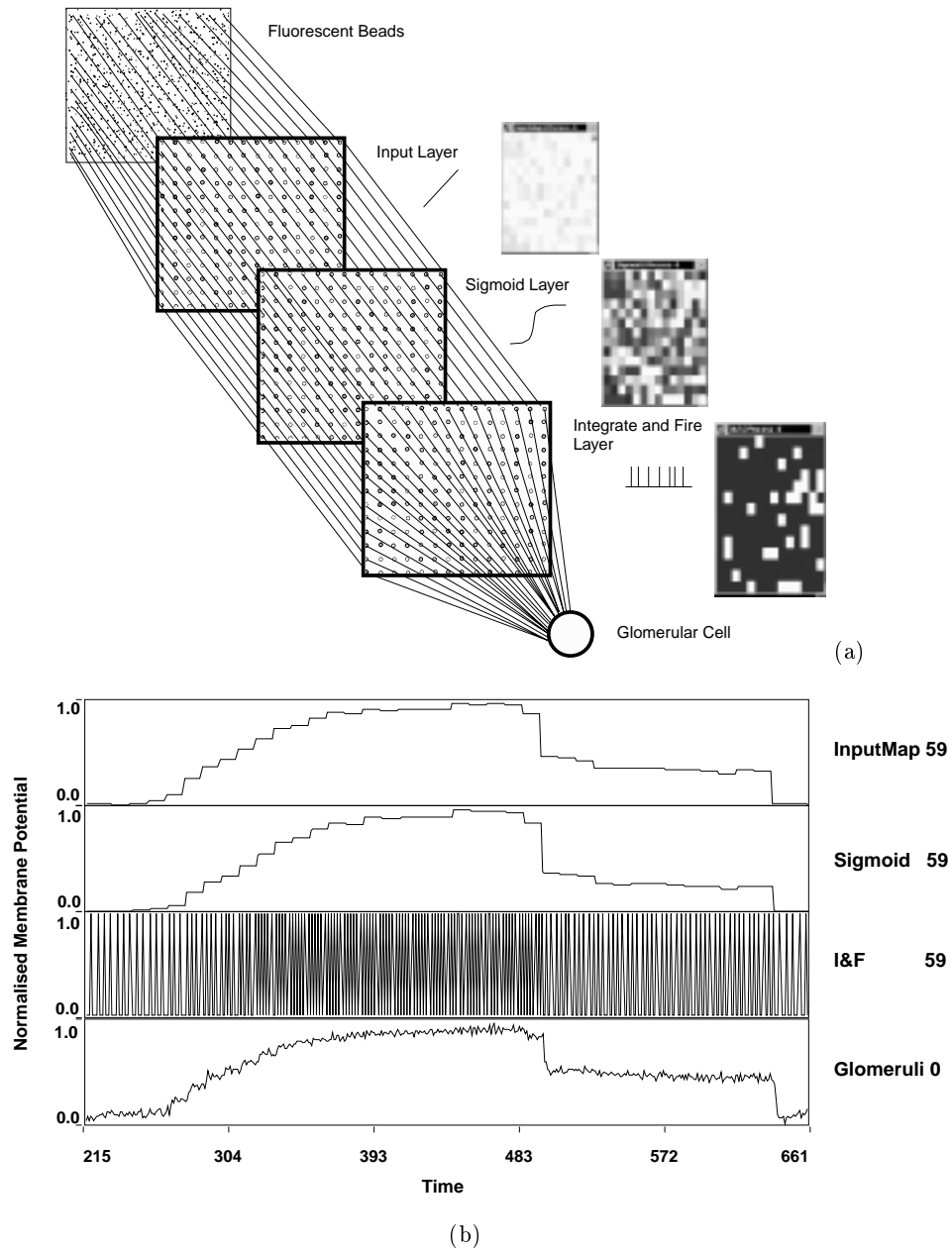


Fig. 7. (a) Architecture of a simple model of the early stages of the olfactory system, showing the different layers, including fluorescent bead population, input layer, sigmoid layer, integrate-and-fire layer, and a single glomerular cell entity. (b) Behaviour of the model over time at each successive stage of the system during a complete cycle of the stimulus – top to bottom: examples of the activity of a single simulated neuron belonging to the input layer responding to the bead response shown in Fig. 3b, sigmoid layer, and integrate-and-fire layer respectively. The bottom trace shows the stimulus after reconstruction from multiple spike trains at the level of the simulated glomerulus.

sigmoid layer in order to mimic the sigmoidal concentration dependence of transduction current within olfactory receptor neurons[24]. This also acts to auto-scale the data so that each bead response lies within the range $[0, 1]$.

Integrate-and-fire neurons were then used to generate a volley of spike trains that represent the stimulus using Poisson statistics as outlined in (1). This arrangement provides a simple yet reasonably accurate model of spike generation by olfactory receptors, which can be considered to produce spike trains with Poisson statistics where the mean firing frequency is sigmoidally dependent upon stimulus concentration. The convergence of receptor input in the biology has been represented in our model by the aggregation of spike trains from many integrate-and-fire cells at any one point in time at the glomerulus "cell". While the glomerulus does not exist as a cell entity in its own right (it comprises neuropil made up from axons from olfactory receptor neurons synapsing onto the dendrites of mitral, tufted, and periglomerular cells), we can use this in our model as a convenient site for integration that represents the excitatory effect of the receptor input on the olfactory bulb.

The behaviour of our model to real-world chemosensory input is shown in Fig. 7b. Here, a single cell in the input layer presents a complete cycle of the luminosity response of an individual microbead. This signal is then compressed by its corresponding cell within the sigmoid layer, and then transformed into a probabilistic spike train at the integrate-and-fire layer. By integrating a large number of such spike trains in both space and time (Fig. 7b, bottom), the glomerular cell is then able to reconstruct the stimulus. The key point to note here is that the signal can only be reconstructed accurately if spikes arrive at random points in time, and that at any point in time the glomerulus is receiving an accurate mean signal from the entire population of chemosensors. The system is therefore dependent upon the massively convergent rate-coded receptor input in order to accurately reconstruct the stimulus.

An important aspect related to how robustly the transmission scheme behaves under realistic input conditions, is how well the glomerulus is able to track the change in the stimulus over time using only discrete spiking input. This issue is central to the performance of any sensory system that must use the input provided from a population of receptors in order to make decisions about the stimulus, such as in the visual and auditory pathways. To estimate the SNR of the reconstructed stimulus, and so quantify the information available to any subsequent neuronal processing within the olfactory pathway, we conducted experiments on two models of the form shown in Fig. 7a in parallel. By comparing the signal produced from a single glomerulus in one model whilst being exposed to air, to an identical model during exposure to 1:10 dilution of saturated toluene vapour, an accurate estimate of the ability of the artificial sensory system to reconstruct the stimulus could be made.

To address the central issue related to robust signal encoding strategies we asked the question, does a rate-coded representation of the stimulus at the receptor level limit the signal quality that is recoverable at the glomerulus? To investigate this issue, we compared the results obtained from two models, one in which probabilistic spike trains representing the receptor input were integrated

at the glomerular cell and another in which the graded (non-spiking) receptor input was transmitted directly to the glomerulus for integration.

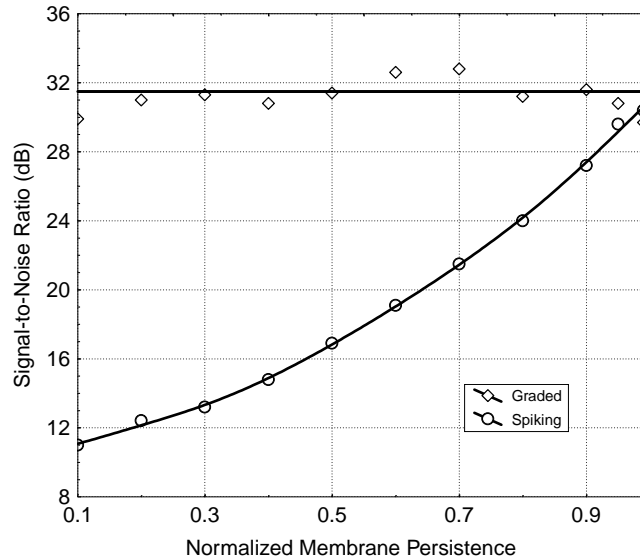


Fig. 8. A comparison of the signal-to-noise ratio obtained at the glomerular cell of our neuronal model for two different encoding schemes – rate-coded spike trains and graded signal transmission.

The results comparing the SNR obtained at the glomerular cell for both operating regimes are shown in Fig. 8. The results demonstrate that direct transmission of graded receptor input gives rise to uniformly high SNR which is robust to variations in the charging time-constant at the glomerulus. For very short time constants the spiking rate-coded equivalent does very poorly, achieving an SNR at the glomerulus that is worse than that of any single receptor. However, for longer integration periods the SNR under the rate-coded regime approaches that achieved during graded signal transmission, showing that a similar efficiency of stimulus encoding can be achieved, but only within a specific range of temporal integration. The cost for adequately recovering a reasonable SNR at the glomerulus in the case of spiking rate-coded stimuli is, though, a far longer integration period, which slows the dynamics of the system as a whole and so limits the response time of the system. If the temporal dynamics of the odorant diffusion through the mucous layer of the olfactory epithelium and signal transduction dynamics at ORNs matched those of the glomeruli there would be no cost to pay since the system would act as a matched filter. Rate-coded stimulus encoding confers clear advantages in terms of its robust properties in the face

of external noise sources, and so is preferable for reliable transmission over long distances such as between the epithelium and the olfactory bulb in the CNS.

These results indicate a clear trade-off between integration time and reconstructed signal quality during spike-based stimulus encoding. This represents an important aspect of how signal integrity can be maintained within a rate-coded regime which is fundamental to understanding the transmission of stimulus information throughout sensory systems.

5 Discussion and Summary

The focus of this chapter has been the robust transmission and reconstruction of sensory signals within neural systems. The olfactory pathway provides an excellent model system from which to address these issues. Two models of the early stages of this system have been presented; a mathematical model of sensitivity enhancement in the olfactory pathway and a computational model for comparing action- and graded-potential based signal transmission. Both models provide insight into aspects of robust signal processing and transmission. Massive convergence of receptor input coupled with population coding brings advantages to the olfactory system by way of fault-tolerance and sensitivity enhancement. Our computational model has demonstrated how spike based communication can be as efficient for signal transmission as graded-potential communication subject to temporal constraints.

How the CNS manages to transmit huge quantities of sensory information to the higher brain centres is a fascinating example of parallel processing. Individual sensory and bulbar neurons may only operate on a millisecond timescale, yet the entire olfactory system is able to make important decisions relating to the stimulus within a remarkable short period of time. Such a feat of information processing requires highly organised strategies to communicate and deal with sensory data in parallel. Investigating key organisation principles within the CNS, such as population coding provides a promising approach to replicating some of the robust properties of signal transmission whilst maintaining high bandwidth or sensory data.

An interesting aspect related to achieving such enormous bandwidth of sensory information that is suggested by our models, and merits further investigation is the matching of dynamics in the time domain of the perireceptor, signal transduction, transmission and processing stages. Further issues that might be investigated using a similar modelling approach are how stimulus and time is represented in the olfactory bulb and in particular the role of temporally complex mitral/tufted cell responses, and oscillations present within the system as a whole[25].

The authors wish to thank Keith Albert and David Walt (Chemistry Department, Tufts University, Boston, MA, USA) for fabricating the optical microbeads used as part of this study. This work was funded by grants from the Royal Society (to TCP/PFMJV), SPP-SNF (to PFMJV), ONR, NIH and DARPA (to JSK).

References

- [1] Singer M.S., Shepherd G.M., Greer C.A., Olfactory receptors guide axons, *Nature* **377** (1995) 19-20.
- [2] Lin D.M., Ngai J., Development of the vertebrate main olfactory system, *Curr. Opin. Neurobiol.* **9** (1999) 74-78.
- [3] Dalton P., Psychophysical and behavioral characteristics of olfactory adaptation, *Chem. Sens.* **25** (2000) 487-492. .
- [4] Christensen T.A., Heinbockel T., Hildebrand J.G., Olfactory information processing in the brain: encoding chemical and temporal features of odors, *J. Neurobiol.* **30** (1996) 82-91.
- [5] Reike R., Warland D, de Ruyter van Steveninck R., and Bialek W., *Spikes: Exploring the Neural Code*, MIT Press: MA, USA, 1997.
- [6] Pearce T.C., Verschure P.F.M.J.V. Olfaction: modeling and experimenting with an artificial nose, in NSF Report: Workshop on Neuromorphic Engineering Telluride, CO, USA. June 1998.
- [7] Kauer, J.S., In: *The Neurobiology of Taste and Smell.* eds: T.E. Finger and W.L. Silver. John Wiley and Sons. pp. 205-231, 1987.
- [8] Vassar R., Chao K.C., Sitcheran R., Nunez J.M., Vosshall L.B., Axel R., Topographic organization of sensory projections to the olfactory-bulb, *Cell* **79** (1994) 981-991.
- [9] Van Drongelen W., Holley A., Doving K.B., Convergence in the olfactory system: quantitative aspects of odour sensing, *J. Theor. Biol.* **71** (1978) 39-48.
- [10] Churchland P.S., Sejnowski T.J., *The Computational Brain*, MIT Press: Cambridge MA., 1992.
- [11] Klein S.A., Levi D.M. Hyperacuity thresholds of 1 sec: theoretical predictions and empirical validation, *J. Opt. Soc. Am. A* **2** (1985) 1170-1190.
- [12] Duchamp-Viret P., Duchamp A., Vigouroux M., Amplifying role of convergence in olfactory system: A comparative Study of receptor cell and second-order neuron sensitivities, *J. Neurophysiol.* **61** (1989) 1085-1095.
- [13] Van Drongelen W., Unitary recordings of near threshold response of receptor cells in the frog, *J. Physiol. London*, **277** (1978) 423-435.
- [14] Boeckh J., Ernst K.D., Contribution of single unit analysis in insects to an understanding of olfactory function, *J. Comp. Physiol. A* **161** (1987) 549-565.
- [15] Mar D.J., Chow C.C., Gerstner W., Adams R.W., Collines J.J., Noise shaping in populations of coupled model neurons, *PNAS* **96** (1999) 10450-10455.
- [16] Dickinson T.A., White J., Kauer J.S., Walt D.R., A chemical-detecting system based on a cross-reactive optical sensor array, *Nature* **382** (1996) 697-700.
- [17] Albert K.J., Lewis N.S., Schauer C.L., Sotzing, G.A., Stitzel S.E., Vaid T.P., Walt D.R., Cross-reactive chemical sensor arrays, *Chem. Rev.* **100** (2000) 2595-2626.
- [18] Dickinson T.A., Michael K.L., Kauer J.S., Walt D.R., Convergent, self-encoded bead sensor arrays in the design of an artificial nose. *Anal. Chem.* **71** (1999) 2192-2198.
- [19] White J., Kauer J.S., Dickinson T.A., Walt D.R., Rapid analyte recognition in a device based on optical sensors and the olfactory system, *Anal. Chem.* **68** (1996) 2191-2202.
- [20] Sharaf M.A., Illman D.L., Kowalski B.R., *Chemometrics*, John Wiley & Sons: New York., 1986.

- [21] Softky W.R., Koch C., The highly irregular firing of cortical cells is inconsistent with temporal integration of random EPSPs, *J. Neurosci.* **13** (1993) 334.
- [22] Mainen Z.F., Sejnowski T.J., Reliability of spike timing in neocortical neurons, *Science* **268** (1995) 1503.
- [23] Shadlen M.N., Newsome W.T., The variable discharge of cortical neurons: implications for connectivity, computation, and information coding, *J. Neuroscience* **18** (1998) 3870.
- [24] Lowe G., Gold G.H., Nonlinear amplification by calcium-dependent chloride channels in olfactory receptor cells, *Nature* **386** 1993 283-286.
- [25] Laurent G., A systems perspective on early olfactory coding, *Science* **286** (1999) 723-728.